1608 *Organometallics* 1988, 7, 1608–1613

Metallo-Selective Substitution Reactions by Amines or Phosphines in $HRuCo_3(CO)_{12}$. IR and ^1H and ^{59}Co NMR Studies of $HRuCo_3(CO)_{12-x}L_x$ (L = Amines or Phosphines; x = 0–2) and Crystal Structure of $HRuCo_3(CO)_{11}(PPh_3)$[†]

Hiroyuki Matsuzaka,[1a] Teruyuki Kodama,[1b] Yasuzo Uchida,[1b] and Masanobu Hidai*[,1a]

Department of Synthetic Chemistry and Department of Industrial Chemistry, Faculty of Engineering, The University of Tokyo, Hongo, Bunkyo-ku, Tokyo 113, Japan

Received January 25, 1988

Reaction of a mixed-metal cluster $HRuCo_3(CO)_{12}$ with trimethylamine *N*-oxide or a series of amines leads to the formation of the amine-substituted clusters of the form $HRuCo_3(CO)_{11}L$ (L = NMe_3, NEt_3, NMe_2Ph, *p*-$H_2N(C_6H_4)NH_2$, 1,4-cyclohexanediamine (1,4-chxn)) in 20–40% yield. The reaction with *N,N,N′,N′*-tetramethylethylenediamine (TMEDA) gives a disubstituted cluster, $HRuCo_3(CO)_{10}$(TMEDA). IR and ^1H and ^{59}Co NMR spectra of these clusters indicate that the substitution of amines for the CO ligand takes place preferentially at the ruthenium atom. On the other hand, the reaction with tertiary phosphines gives the phosphine-substituted clusters $HRuCo_3(CO)_{12-x}L_x$ (L = PPh_3, x = 1, 2; L = (diphenylphosphino)ethane (dppe), x = 1) in 70–90% yield, where the substitution of phosphines occurs exclusively at the cobalt atom. The structure of $HRuCo_3(CO)_{11}(PPh_3)$ has been determined by X-ray diffraction. It crystallizes in the space group $P2_1/c$ with a = 11.940 (4) Å, b = 17.103 (6) Å, c = 17.431 (7) Å, β = 118.55 (3)°, and Z = 4. The structure is refined to R_1 = 0.0801 and R_2 = 0.101 for 3980 independent reflections having $F_o > 3\sigma(F_o)$. The cluster has a tetrahedral structure similar to that of the parent $HRuCo_3(CO)_{12}$ cluster, and the phosphine ligand is axially bonded to one of the three basal cobalt atoms.

Introduction

An extensive chemistry of transition-metal clusters has recently been developed, and numerous reviews on their various aspects have appeared.[2] In particular, mixed-metal clusters are currently under intensive investigation because unique catalysis is expected, owing to the possible different site reactivities.

We have previously reported the synthesis and structure determination of the mixed-metal clusters $M[RuCo_3(CO)_{12}]$ (M = Na, Et_4N, Ph_4P, $(Ph_3P)_2N$, and H)[3] and their catalytic activities for homlogation of methanol[3] and methyl acetate[4] and hydroformylation of olefins.[5] During the course of our study on the reactivities of the above mixed-metal clusters, we recently have found metallo-selective substitution reactions of amines or phosphines for the carbonyl ligand in $HRuCo_3(CO)_{12}$.[6] To our knowledge, this is one of a few examples in which reactions with similar substrates occur at different specific locations on mixed-metal clusters.[7] This was briefly reported in a previous paper. We describe here the full details of the synthesis of amine- or phosphine-substituted clusters $HRuCo_3(CO)_{12-x}L_x$ (L = amines or phosphines, x = 1 or 2) and their characterization by IR and ^1H and ^{59}Co NMR spectroscopy as well as an X-ray structural analysis of $HRuCo_3(CO)_{11}(PPh_3)$.

Scheme I

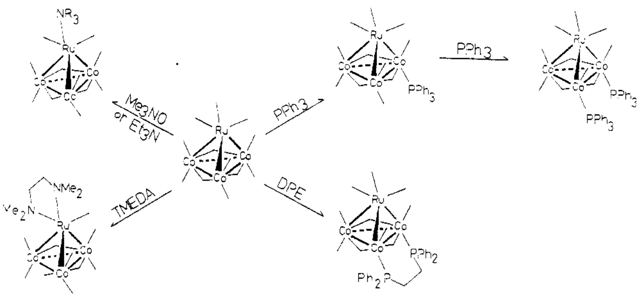

Results and Discussion

Preparation of Amine- or Phosphine-Substituted Clusters. Reaction of the mixed-metal cluster $HRuCo_3(CO)_{12}$ (**1**) with 1 molar equiv of trimethylamine *N*-oxide in dichloromethane at room temperature leads to the formation of an amine-substituted cluster, $HRuCo_3(CO)_{11}(NMe_3)$ (**2**), in moderate yield concurrent with evolution of CO_2 (which is substantiated by observing a white precipitate when the gaseous product is treated with an aqueous solution of $Ba(OH)_2$). A series of amine-substituted clusters, $HRuCo_3(CO)_{11}L$ (**3**, L = NEt_3; **4**, L = Me_2NPh; **5**, L = *p*-$H_2N(C_6H_4)NH_2$; **6**, L = 1,4-cyclohexanediamine (1,4-chxn)), were prepared by direct treatment of **1** with an equivalent amount of amines (Scheme I). Evolution of CO was observed during the reaction, the amount of which was estimated to be ca. 0.7

[†] Part 8 of the series "The Chemistry of Heteronuclear Clusters and Homogeneous Multimetallic Catalysts". For part 7, see ref 6.

(1) (a) Department of Synthetic Chemistry. (b) Department of Industrial Chemistry.

(2) (a) Roberts, D. A.; Geoffroy, G. L. *Comprehensive Organometallic Chemistry*; Willkinson, G., Stone, F. G. A., Abel, E. W., Eds.; Pergamon: Oxford, 1982; Vol. 6. (b) Gladfelter, W. L.; Geoffroy, G. L. *Adv. Organomet. Chem.* **1980**, *18*, 207. (c) Johnson, B. F. G., Ed. *Transition Metal Clusters*; Wiley-Interscience: New York, 1980. (d) Gates, B. C.; Guczi, L.; Knozinger, H., Ed. *Metal Clusters in Catalysis*; Elsevier: New York, 1986.

(3) Hidai, M.; Orisaku, M.; Ue, M.; Koyasu, Y.; Kodama, T.; Uchida, Y. *Organometallics* **1983**, *2*, 292.

(4) Hidai, M.; Koyasu, Y.; Yokota, M.; Orisaku, M.; Uchida, Y. *Bull. Chem. Soc. Jpn.* **1982**, *55*, 3951.

(5) Hidai, M.; Fukuoka, A.; Koyasu, Y.; Uchida, Y. *J. Mol. Catal.* **1986**, *35*, 29.

(6) Hidai, M.; Matsuzaka, H.; Koyasu, Y.; Uchida, Y. *J. Chem. Soc., Chem. Commun.* **1986**, *1451*.

(7) For some pertinent examples see: (a) Horvath, I. T.; Zsolnai, L.; Huttner, G. *Organometallics* **1986**, *5*, 180. (b) Balch, A. L.; Linehan, J. C.; Olmstead, M. M. *Inorg. Chem.* **1985**, *24*, 3975. (c) Fox, J. R.; Gladfelter, W. L.; Wood, T. G.; Smegal, J. A.; Foreman, T. K.; Geoffroy, G. L.; Tavanaiepour, I.; Day, V. W.; Day, C. S. *Ibid.* **1981**, *20*, 3214. (d) Dalton, D. M.; Barnett, D. J.; Duggan, T. P.; Keister, J. B.; Malik, P. T.; Modi, S. P.; Shaffer, M. R.; Smesko, S. A. *Organometallics* **1985**, *4*, 1854. (e) Roland, E.; Vahrenkamp, H. *Ibid.* **1983**, *2*, 183. (f) Huie, B. T.; Knobler, C. B.; Kaesz, H. D. *J. Am. Chem. Soc.* **1978**, *100*, 3059. (g) Johnston, P.; Hutchings, G. J.; Denner, L.; Boeyens, J. C. A.; Coville, N. L. *Organometallics* **1987**, *6*, 1292.

0276-7333/88/2307-1608$01.50/0

Table I. Infrared Spectra of Amine- or Phosphine-Substituted Clusters 1–10 in the ν(CO) Region

compounds	ν(CO) (cm^{-1}; CH_2Cl_2)
$HRuCo_3(CO)_{12}$ (**1**)	2062 s, 2021 m, 1877 m
$HRuCO_3(CO)_{11}(NMe_3)$ (**2**)	2060 w, 2018 s, 2005 s, 1971 m, 1811 m
$HRuCo_3(CO)_{11}(NEt_3)$ (**3**)	2065 w, 2020 s, 2006 s, 1815 m
$HRuCo_3(CO)_{11}(NMe_2Ph)$ (**4**)	2060 s, 2000 s, 1997 m, 1878 m
$HRuCo_3(CO)_{11}(p\text{-}H_2NC_6H_4NH_2)$ (**5**)	2053 m, 2000 s, 1994 s, 1976 m, 1802 m
$HRuCo_3(CO)_{11}$(1,4-chxn) (**6**)	1997 s, 1977 m, 1810 m
$HRuCo_3(CO)_{10}$(TMEDA) (**7**)	2066 w, 2019 s, 2003 s, 1970 m, 1812 m
$HRuCo_3(CO)_{11}(PPh_3)$ (**8**)	2081 m, 2045 s, 2008 s, 1861 m, 1846 m
$HRuCo_3(CO)_{10}(PPh_3)_2$ (**9**)	2060 s, 2004 s, 1996 s, 1951 m, 1838 m, 1830 m
$HRuCo_3(CO)_{10}$(dppe) (**10**)	2070 s, 2002 s, 1949 s, 1843 m, 1805 m

mol/cluster by GSC. Even if a large excess of amine or amine oxide is used and/or the reaction temperature is raised to 70 °C, only the same monosubstituted clusters are obtained. This indicates that the products are thermodynamically determined. The above reaction is in sharp contrast to the substitution reaction of the cluster **1** with triphenylphosphine which gives a disubstituted cluster under appropriate conditions (vide infra). Substitution of amines, which are stronger σ-donors than phosphines, increases π-back-donation from the metal to the remaining carbonyls. This results in stronger metal–carbonyl bonds and prevents further substitution by amines. Actually, the bands assigned to ν(CO) in the IR spectra of the amine-substituted clusters shift to lower frequencies compared with those of the phosphine-substituted clusters (Table I). Substitution of amine for the two CO ligands in **1** proceeds only when the bidentate ligand $Me_2NCH_2CH_2NMe_2$ (TMEDA) is used and the disubstituted cluster $HRuCo_3(CO)_{10}$(TMEDA) (**7**) is obtained.

Treatment of **1** with 1 molar equivalent of PPh_3 in dichloromethane gives a monosubstituted cluster, $HRuCo_3(CO)_{11}(PPh_3)$ (**8**), in 90% yield, which reacts further with another PPh_3 to give a disubstituted cluster, $HRuCo_3(CO)_{10}(PPh_3)_2$ (**9**). Complex **9** is also obtained in high yield by direct treatment of **1** with 3 molar equiv of PPh_3. Reaction of **1** with 1 molar equiv of $Ph_2PCH_2CH_2PPh_2$ (dppe) leads to the formation of $HRuCo_3(CO)_{10}$(dppe) (**10**) in 69% yield. Previously, Pakkanen and co-workers reported preparation of **9**[8] and **10**[9] by the benzophenone ketyl catalyzed reaction of **1** with PPh_3 and dppe in THF, respectively, but the yields were relatively low (25–47%) and several byproducts were formed. It is of great interest to note that the same reactions using dichloromethane as a solvent proceed smoothly without any catalyst and lead to formation of **9** and **10** in high yields (70–90%).

The substitution reaction of $HFeCo_3(CO)_{12}$, which is isostructural with **1**, with various phosphorus donor ligands was previously investigated by Mays and co-workers, and a series of substituted clusters, $HFeCo_3(CO)_{12-x}L_x$ (x = 1–4; L = phosphine or phosphite), were prepared.[10] However, similar substitution reactions of the mixed-metal cluster with amines do not proceed because the hydride cluster has much more acidic character than cluster **1**, and the ammonium salts $[R_3NH][FeCo_3(CO)_{12}]$ are obtained.[11,12]

Table II. ^{1}H and ^{59}Co NMR Data for Amine- or Phosphine-Substituted Clusters 1–10

compds	^{1}H NMR[a] (δ)	^{59}Co NMR[b] (δ)
1	−19.4	−2648 [−2464, −2514, −2768]
2	−17.2	−2649
3	−17.2	−2630
4	−17.1	−2649
5	−17.3	−2650
6	−17.2	−2649
7	−17.4	−2649
8	−19.4	−2574 (1), −2712 (2) [−2461, −2648]
9	−19.7	−2575 (1), −2715 (2) [−2350]
10	−20.1	−2713 −2745 sh [−2467, −2648]

[a] Chemical shifts values of metal hydride peaks in CD_2Cl_2 recorded at 27 °C relative to Me_4Si. [b] In acetone-d_6 solution recorded at 27 °C. Measured from an aqueous solution of $K_3[Co(CN)_6]$ as an external standard. [c] The peaks in brackets are quite minor. [d] Intensity ratio in parentheses.

The corresponding ruthenium analogue $[Et_3NH][RuCo_3(CO)_{12}]$ is obtained in moderate yield by treatment of $Na[RuCo_3(CO)_{12}]$ with $[Et_3NH]Cl$ in water. The ^{1}H NMR spectrum of $[Et_3NH][RuCo_3(CO)_{12}]$ shows one set of signals characteristic of the $[Et_3NH]^+$ cation (3.66 (CH_2, quartet), 1.9 ppm, (CH_3, t)). This is completely different from that of $HRuCo_3(CO)_{11}(NEt_3)$ (vide infra).

Anionic clusters $M[RuCo_3(CO)_{12}]$ (M = Na, Et_4N) do not react with amines or trimethylamine *N*-oxide under the same conditions. It seems plausible that stronger metal–carbonyl bonds in the anionic clusters caused by an increase of the π-back-donation from the metal to the carbonyl ligands prohibit the substitution reactions with amines.

Characterization of Amine- or Phosphine-Substituted Clusters. Spectroscopic data for **1**–**10** are given in Tables I and II. Substitution of electron-donating amines or phosphines for the carbonyl ligands results in lower shifts of ν(CO) in the IR spectra. The bands due to ν(CO) of the amine-substituted clusters appear at lower frequencies than those of phosphine-substituted clusters. Furthermore, it is of great interest that the IR spectra of amine-substituted clusters in the ν(CO) region are quite different from those of phosphine-substituted clusters. For example, the amine-substituted cluster **2** shows one medium peak at 1811 cm^{-1} characteristic of a bridging carbonyl group, whereas the phosphine-substituted cluster **8** exhibits two medium peaks at 1861 and 1846 cm^{-1} assigned to bridging carbonyl groups. The pattern of terminal ν(CO) bands is also quite different. This strongly suggests that the site for the substitution of amines and phosphines in cluster **1** may be different.

Kaesz et al. demonstrated unequivocally that the hydride in $HFeCo_3(CO)_9[P(OMe)_3]_3$ is located on the Co_3 face by a neutron diffraction study.[7f] Recently, Saito and Sawada observed ^{1}H NMR spectra of $HFeCo_3(CO)_{12}$ and **1** in a $Fe(CO)_5$–toluene-d_8 mixed solvent, which showed broad singlets at −21.1 and −19.4 ppm, respectively. The line width became narrower on lowering the temperature when the relaxation time T_1 of cobalt became much smaller, and the hydride resonance was effectively decoupled.[13] As these spectral features were similar to those of $HFeCo_3(CO)_9[P(OMe)_3]_3$, the hydride ligands in $HFeCo_3(CO)_{12}$ and **1** were assumed to be μ_3-bonded to the Co_3 face. The ^{1}H NMR spectra of amine-substituted clusters **2**–**6** show a broad singlet at −17.1 to −17.4 ppm charac-

---

(8) Pursiainen, J.; Pakkanen, T. A. *J. Organomet. Chem.* **1985**, *290*, 85.

(9) Pursiainen, J.; Pakkanen, T. A. *J. Organomet. Chem.* **1986**, *309*, 187.

(10) Cooke, C. G.; Mays, M. J. *J. Chem. Soc., Dalton Trans.* **1975**, 455.

(11) Chini, P. *Gazz. Chim. Ital.* **1960**, *90*, 1005.

(12) Nishihara, H.; Mori, T.; Tsurita, Y.; Nakano, K.; Saito, T.; Sasaki, Y. *J. Am. Chem. Soc.* **1982**, *104*, 4367.

(13) Saito, T.; Sawada, S. *Bull. Chem. Soc. Jpn.* **1985**, *58*, 459..

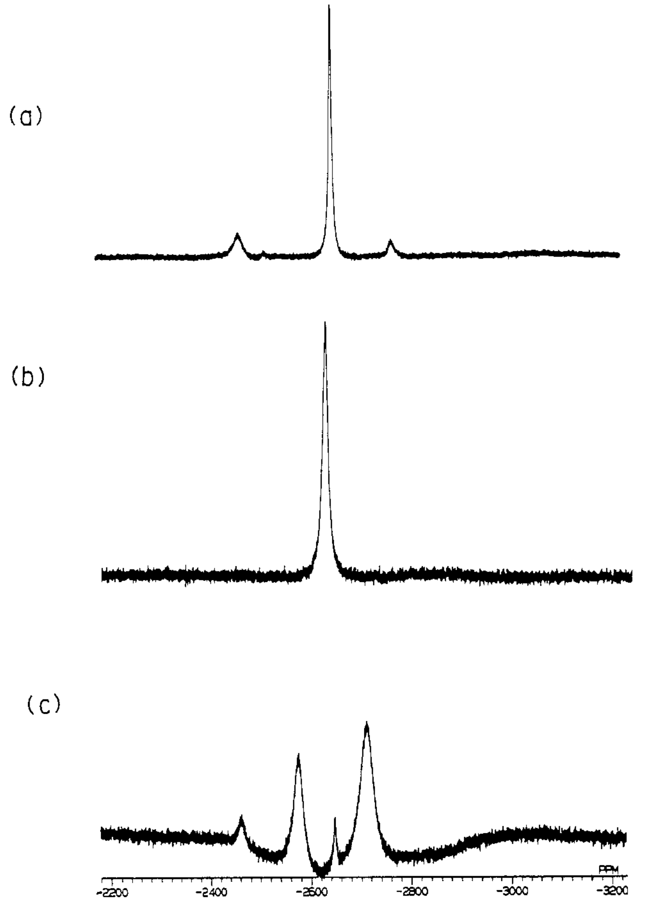

Figure 1. ^{59}Co NMR spectra of amine- or phosphine-substituted clusters: (a) $HRuCo_3(CO)_{12}$ (1), (b) $HRuCo_3(CO)_{11}(NMe_3)$ (2), and (c) $HRuCo_3(CO)_{11}(PPh_3)$ (8) (measured by using an aqueous solution of $K_3[Co(CN)_6]$ as an external standard).

teristic of a metal hydride. The line width becomes narrower as the temperature is lowered.[14] These observations suggest that the hydride in the amine-substituted clusters **2**–**6** is also μ_3-bonded to the Co_3 face. The ^{1}H NMR spectrum of **3** in the presence of free triethylamine exhibits two sets of distinct peaks assigned to the coordinated amine (3.31 (q), 1.46 (t)) and free amine (2.95 (q), 1.26 ppm (t)). This indicates that exchange between the coordinated amine and free amine does not occur on the NMR time scale at ambient temperature (vide infra).[15]

^{59}Co NMR spectra were measured in order to determine whether substitution by amines takes place at the ruthenium or the cobalt atom. Typical spectra are shown in Figure 1. Clusters **2**–**7** show only one peak at −2630 to −2650 ppm in the ^{59}Co NMR spectra which is similar to that of the parent cluster **1**.[16] Furthermore, the line-width signal at half-height ($w_{h/2}$) of the ^{59}Co single resonance (670–770 Hz) is almost the same as that of the parent cluster **1** (740 Hz). This strongly suggests that the symmetry of the electric field around the Co nuclei in clusters **2**–**7** is not essentially changed compared with that of cluster **1**. Although we could not obtain single crystals of **2**–**7** suitable for X-ray structural analysis, the above findings lead to the conclusion that the amine substitution takes place at the ruthenium atom and the hydride ligand is probably μ_3-bonded to the Co_3 face.

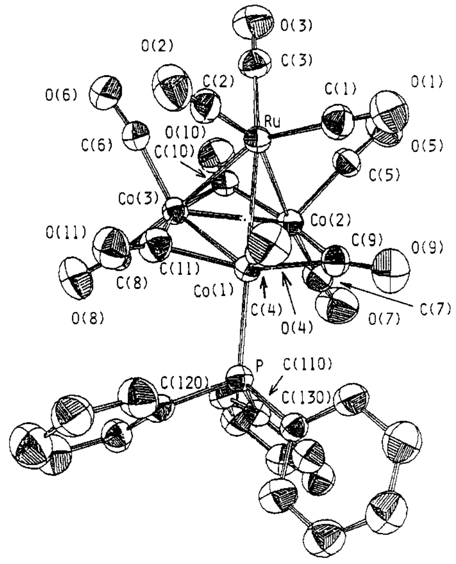

Figure 2. An ORTEP drawing of $HRuCo_3(CO)_{11}(PPh_3)$ (8).

^{1}H NMR spectra of phosphine-substituted clusters **8** and **9** exhibit a broad singlet at −19.4 to −19.7 ppm assigned to the metal hydride. In the ^{59}Co NMR spectrum of **8**, two strong peaks at −2574 and −2712 ppm appear with intensity ratio 1:2, indicating that the phosphine substitution reaction takes place at the cobalt atom.[17] Furthermore, the line-width signals at half-height ($w_{h/2}$) of the two peaks (2280 and 3080 Hz, respectively) are markedly broader than those of the parent cluster **1** and the amine-substituted clusters **2**–**6**. This line broadening probably can be attributed to a decrease of the symmetry of the electric field around the Co nuclei caused by phosphine substitution at the cobalt atom. Similar line broadening was also observed in the ^{59}Co NMR spectrum of $HFeCo_3(CO)_{11}[P(OMe)_3]$, in which $P(OMe)_3$ was axially coordinated to one of the three basal cobalt atoms.[7f,10,18] The $w_{h/2}$ value of the single resonance for $HFeCo_3(CO)_{12}$ was 674 Hz, whereas those of the two resonances with intensity ratio 1:2 for $HFeCo_3(CO)_{11}[P(OMe)_3]$ were 1304 and 2065 Hz, respectively.[13]

Previously, Milone et al.[18] observed variable-temperature ^{13}C NMR spectra of $HFeCo_3(CO)_{12-x}L_x$ (L = PPh_3 or $P(OPh)_3$; x = 0–3), which revealed that the molecule $HFeCo_3(CO)_{12}$ was stereochemically nonrigid and that the carbonyls bonded to the iron atom were not engaged in delocalized scrambling of the bridging and terminal carbonyls in the basal Co_3 moiety. They also showed that the cobalt-bonded carbonyls were relatively rigid in the substituted clusters $HFeCo_3(CO)_{12-x}L_x$. We could observe here the ^{13}C NMR spectrum of **1**, but ^{13}C NMR spectra of amine- or phosphine-substituted clusters **2**–**10** could, unfortunately, not be observed because of their poor solubility. The ^{13}C NMR spectrum of **1** exhibits three peaks at 202.7, 198.9, and 190.7 ppm at −60 °C. The $w_{h/2}$ values

---

(14) For example, the line-width signals at half-height ($w_{h/2}$) for **2** at 27 and −60 °C are 110 and 35 Hz, respectively.

(15) Variable-temperature ^{1}H NMR spectra of **3** in the presence of free triethylamine (ca. 6 equiv) were also measured. When the temperature was raised to 55 °C, the signals assigned to the coordinated amine significantly broadened. This indicates that exchange between the coordinated amine and free amine occurs on the NMR time scale at this temperature.

(16) The existence of a small amount of an isomer in solution is shown by a variable-temperature ^{1}H NMR study of **1** (see ref 13). A weak and sharp line at −19.9 ppm overlapped on the broad main peak at −19.9 ppm was observed when the temperature was lowered to −50 °C. The existence of isomers is also supported by the ^{59}Co NMR spectrum that shows weak peaks at −2464, −2514, and −2768 ppm in addition to a strong peak at −2648 ppm.

(17) The existence of a small amount of isomers in solution is shown by the observation of weak peaks at −2461 and −2648 ppm in addition to the above strong peaks.

(18) Aime, S.; Milone, L.; Osella, D.; Poli, A. *Inorg. Chim. Acta* **1978**, *30*, 45.

Table III. Selected Bond Distances (Å) and Angles (deg) of $HRuCo_3(CO)_{11}(PPh_3)$ (8)

Bond Distances

Ru–Co1	2.649 (3)	Ru–Co2	2.631 (3)	Ru–Co3	2.630 (3)
Co1–Co2	2.533 (4)	Co2–Co3	2.517 (4)	Co3–Co1	2.527 (4)
Ru–C1	1.91 (2)	Ru–C2	1.90 (2)	Ru–C3	1.91 (2)
Co1–P	2.261 (5)	Co1–C4	1.76 (2)	Co2–C5	1.76 (2)
Co3–C6	1.79 (2)	Co2–C7	1.80 (2)	Co3–C8	1.77 (2)
Co1–C9	1.92 (2)	Co2–C9	2.00 (2)	Co2–C10	1.92 (2)
Co3–C10	1.98 (2)	Co3–C11	1.97 (2)	Co1–C11	1.98 (2)
C1–O1	1.16 (3)	C2–O2	1.15 (3)	C3–O3	1.14 (3)
C4–O4	1.14 (3)	C5–O5	1.13 (3)	C6–O6	1.11 (3)
C7–O7	1.14 (3)	C8–O8	1.16 (3)	C9–O9	1.20 (3)
C10–O10	1.17 (3)	C11–O11	1.16 (3)		

Bond Angles

Ru–Co1–Co2	60.98 (9)	Ru–Co1–Co3	61.02 (9)
Ru–Co2–Co1	61.70 (9)	Ru–Co2–Co3	61.41 (9)
Ru–Co3–Co1	61.78 (9)	Ru–Co3–Co2	61.45 (9)
Co1–Ru–Co2	57.32 (8)	Co1–Ru–Co3	57.19 (8)
Co2–Ru–Co3	57.15 (9)	Co1–Co2–Co3	60.06 (10)
Co2–Co3–Co1	60.29 (10)	Co3–Co1–Co2	59.65 (10)
Ru–Co1–C4	84.2 (7)	Ru–Co2–C5	77.5 (7)
Ru–Co3–C6	75.3 (7)	Ru–Co2–C7	175.1 (7)
Ru–Co3–C8	174.6 (7)	Ru–Co1–P	175.0 (2)
Co1–Ru–C1	100.4 (7)	Co1–Ru–C2	101.9 (7)
Co1–Ru–C3	154.5 (7)	Co2–Ru–C1	103.2 (7)
Co2–Ru–C2	155.4 (7)	Co2–Ru–C3	95.4 (9)
Co3–Ru–C1	155.2 (7)	Co3–Ru–C2	101.8 (7)
Co3–Ru–C3	101.1 (7)	Co1–Co2–C5	125.8 (7)
Co3–Co2–C5	128.3 (7)	Co1–Co2–C7	118.6 (7)
Co3–Co2–C7	123.3 (7)	Co2–Co3–C6	124.4 (7)
Co1–Co3–C6	126.1 (7)	Co2–Co3–C8	123.9 (7)
Co1–Co3–C8	119.3 (7)	Co2–Co1–C4	134.7 (7)
Co3–Co1–C4	128.8 (7)	Co2–Co1–P	114.3 (2)
Co3–Co1–P	115.6 (2)	Co1–Co2–C9	48.5 (6)
Co2–Co1–C9	51.0 (6)	Co2–Co3–C10	48.8 (5)
Co3–Co2–C10	51.0 (6)	Co3–Co1–C11	50.2 (7)
Co1–Co3–C11	50.3 (7)	Ru–C1–O1	177 (2)
Ru–C2–O2	177 (2)	Ru–C3–O3	171 (2)
Co1–C4–O4	177 (2)	Co2–C5–O5	173 (2)
Co3–C6–O6	170 (2)	Co2–C7–O7	175 (2)
Co3–C8–O8	170 (2)	Co1–P–C110	114.1 (6)
Co1–P–C120	112.7 (7)	Co1–P–C130	117.5 (6)

for each signals are 28, 10, and 34 Hz, respectively. When the temperature was raised to 22 °C, the broader signals at 202.7 and 190.7 ppm, which are assigned to the COs bound to the cobalt atoms (which have a quadrupole moment), coalesce to one broad peak at 191.2 ppm ($w_{h/2}$) = 60 Hz), whereas the signal at 198.9 ppm remains sharp ($w_{h/2}$ = 10 Hz). The latter signal is probably assigned to the carbonyls bonded to the ruthenium atom. This spectral change shows good accordance with that observed for $HFeCo_3(CO)_{12}$. Thus, the carbonyls bonded to the ruthenium atom are not engaged in delocalized scrambling of the bridging and terminal carbonyls in the basal Co_3 moiety as in the case of $HFeCo_3(CO)_{12}$.

The molecular structure of 8 has been determined by X-ray diffraction and shown in Figure 2. Selected bond distances and angles are listed in Table III. Figure 2 clearly shows that the cluster has a tetrahedral structure and the phosphine ligand is axially coordinated to one of the three basal cobalt atoms with a Co–P bond distance of 2.261 Å. The average value of the Ru–Co–C equatorial carbonyl angles (79.6°) is small enough to exclude the possibility of an edge-bridging hydride in the Ru–Co bonds. The corresponding angles for the hydride-bridged bonds in $H_2Ru_2Co_2(CO)_{12}$ (111.2°)[7e] and $H_2Ru_2Rh_2(CO)_{12}$ (110.7° and 115.8°)[8] are much higher. The hydride ligand of 8 is probably μ_3-bonded to the Co_3 face because the average value of the Co–Co–C axial carbonyl angles (121.6°) is relatively large. The observed average values for non-hydrogen compounds are, for example, 113.1° in $[PPN][RuCo_3(CO)_{12}]$[3] and 105.1° in $Co_4(CO)_{12}$.[19]

Table IV. Yields and Analytical Data of 2–10

		found			calcd		
compds	yields[a] (%)	C	H	N	C	H	N
2	38	25.67	2.00	2.21	26.02	1.56	2.17
3	33	29.46	2.28	1.87	29.67	2.35	2.03
4	28	31.13	1.79	1.69	32.22	1.71	1.98
5	22	30.49	1.56	4.64	29.90	1.26	3.87
6	27	28.91	3.08	3.97	29.12	2.16	3.99
7	34	29.44	2.44	3.75	29.42	2.81	4.03
8	90	41.18	1.85		41.01	1.90	
9	72	50.41	1.82		50.99	1.89	
10	70	45.18	2.79		45.16	2.64	

[a] After recrystallization.

The ^{59}Co NMR spectrum of **9** shows two strong peaks at −2575 and −2715 ppm, with an intensity ratio of 1:2 and $w_{h/2}$ values of 2490 and 2690 Hz, respectively. Recently, Pakkanen et al. have determined the crystal structure of **9** in which each phosphine ligand is axially coordinated to two different cobalt atoms and the hydrogen is triply bridged to the Co_3 face.[8]

Reactions of amine-substituted clusters with PPh_3 did not proceed at ambient temperature. Thus, neither **8** nor a product structurally analogous to **3** was obtained by treatment of **3** with 1 molar equiv of PPh_3, and only **3** was recovered from the reaction mixture. This result shows that dissociation of coordinated amines does not occur at ambient temperature (vide supra). Substitution reactions by amines or phosphines in **1** under UV irradiation resulted in the formation of the same products as those described above. This suggests that both amine and phosphine substitution proceeds by the same mechanism, probably involving CO dissociation. However, we must await further investigations to understand why such metallo-selective substitutions occur.

The bidentate ligands TMEDA and dppe also show a quite different reactivity toward the substitution for the carbonyl ligands in **1** (Scheme I). The ^1H NMR spectrum of the TMEDA-substituted cluster **7** shows only one set of singlets at 2.99 and 2.72 ppm with an intensity ratio of 4:12, which are assigned to methylene and methyl protons in the coordinated TMEDA, respectively. The metal hydride resonance appears at −17.4 ppm as a broad peak. The ^{59}Co NMR spectrum of **7** exhibits one resonance at −2649 ppm with the $w_{h/2}$ value 770 Hz. These results suggest that TMEDA chelates around the ruthenium atom and the hydride ligand is probably μ_3-bonded to the Co_3 face. As for the dppe-substituted cluster **10**, Pakkanen and Pursiainen have recently determined the molecular structure, where dppe is axially coordinated to two different cobalt atoms.[9]

Experimental Section

All manipulations were carried out under a dry nitrogen atmosphere by using standard Schlenk tube techniques. All solvents and reagents were purified by conventional methods and distilled under a nitrogen atmosphere. The compounds PPh_3, $Me_3NO\cdot 2H_2O$, and TMEDA were obtained commercially and used without further purification, while the compounds $HRuCo_3(CO)_{12}$,[3] $HFeCo_3(CO)_{12}$,[20] and dppe[21] were prepared by published method. IR spectra were measured on a Shimazu IR-408 spectrometer. NMR spectra were obtained on a JEOL GX-400 spectrometer operating at 399.8 MHz for ^1H, 100.5 MHz for ^{13}C, and 94.602 MHz for ^{59}Co. Chemical shifts were reported downfield from the internal reference tetramethylsilane for ^1H and ^{13}C and downfield from the external reference an aqueous solution of $K_3[Co(CN)_6]$ for ^{59}Co. In order for variable-temperature ^{13}C NMR spectra to

---

(19) Wei, C. H. *Inorg. Chem.* **1969**, *8*, 2384.
(20) Knight, J.; Mays, M. J. *J. Chem. Soc. A* **1970**, 711.
(21) Chatt, J.; Hart, F. A. *J. Chem. Soc.* **1960**, 1378.

Table V. Crystallographic Data for $HRuCo_3(CO)_{11}(PPh_3)$ (8)

formula	$C_{29}H_{16}O_{11}PRuCo_3$
fw	849.28
cryst syt	monoclinic
space group	$P2_1/c$
a, Å	11.940 (4)
b, Å	17.103 (6)
c, Å	17.431 (7)
β, deg	118.55 (3)
V, Å^3	3126 (7)
Z	4
D_{calcd}, g·cm^{-3}	1.80
D_{obsd}, g·cm^{-3}	1.83 (6)^a
λ(Mo Kα), Å	0.71069
scan type	$2\theta-\omega$
scan width, deg	1.0 + 0.45 tan θ
data collctn range	$1.25 < \theta < 30.0°$
no. of unique data	9418
no. of data, $F_o > 3\sigma(F_o)$	3980
no. of refined variables	467
$R_1 = \sum\|\|F_o\| - \|F_c\|\|/\sum\|F_o\|$	0.0801
$R_2 = [\sum w(\|F_o\| - \|F_c\|)^2/\sum w\|F_o\|^2]^{1/2}$	0.101

^{a} Flotation in an aqueous zinc chloride solution.

be obtained, $HRuCo_3(CO)_{12}$ (1) was enriched by stirring for some days in a sealed ampule at room temperature in the presence of <1 atm of 90% enriched ^{13}CO (Merk & Co., Inc.). Yields and elemental analysis data for **2**–**10** are presented in Table IV.

Preparation of $HRuCo_3(CO)_{11}(NMe_3)$ (2). A solution of $Me_3NO{\cdot}2H_2O$ (0.0449 g, 0.445 mmol) in CH_2Cl_2 (10 mL) was added to a solution of $HRuCo_3(CO)_{12}$ (1) (0.294 g, 0.478 mmol) in CH_2Cl_2 (10 mL). Evolution of CO_2 occurred immediately. This was substantiated by observing a white precipitate when the gas evolved was bubbled into a $Ba(OH)_2$ solution. The reaction mixture was stirred at room temperature for 4 h during which a small amount of solid precipitated. After the solution was filtered, the solvent was evaporated in vacuo and the resulting solid was recrystrallized from THF (5 mL)–hexane (10 mL) to give the title compound as reddish brown crystals, which were washed with hexane and dried in vacuo (0.117 g, yield 38%).

Preparation of $HRuCo_3(CO)_{11}(NEt_3)$ (3). To a suspension of 1 (0.285 g, 0.339 mmol) in THF (10 mL) was added NEt_3 (0.0350 g, 0.347 mmol), and the reaction mixture was stirred at room temperature for 1 day. The system became homogeneous as the reaction proceeded. After the solvent was evaporated in vacuo, the resulting residue was recrystallized from THF (5 mL)–hexane (10 mL) to give the title compound as needlelike dark red crystals, which were washed with hexane and dried in vacuo (0.077 g, yield 33%).

Other amine-substituted clusters, **4**–**7**, were similarly prepared.

Preparation of $HRuCo_3(CO)_{11}(PPh_3)$ (8). Cluster 1 (0.212 g, 0.345 mmol) and PPh_3 (0.0925 g, 0.353 mmol) were dissolved in CH_2Cl_2 (20 mL), and the mixture was stirred at room temperature for 4 h. Addition of hexane to a concentrated dark violet solution gave the title compound as violet cubic crystals (0.336 g, yield 90%).

Preparation of $HRuCo_3(CO)_{10}(PPh_3)_2$ (9). Cluster 8 (0.103 g, 0.121 mmol) and PPh_3 (0.074 g, 0.282 mmol) was dissolved in CH_2Cl_2 (20 mL), and the solution was refluxed for 8 h. Addition of hexane to a concentrated dark violet solution gave the title compound as violet crystals (0.092 g, yield 90%). The title compound was also obtained by direct reaction of 1 with 3 molar equiv of PPh_3 in CH_2Cl_2 at refluxing temperature.

Preparation of $HRuCo_3(CO)_{10}$(dppe) (10). A solution of 1 (0.303 g, 0.493 mmol) and dppe (0.200 g, 0.600 mmol) in CH_2Cl_2 (20 mL) was refluxed for 8 h. The title compound was obtained analogously as described above.

Table VI. Atomic Parameters (×10^4) and Equivalent Isotropic Temperature Factors (×10)

atom	x	y	z	B_{eq},^{a} Å^2
Ru	−2984 (1)	2030 (1)	2253 (1)	2.8
Co1	−5350 (2)	2507 (1)	1224 (1)	2.5
Co2	−4933 (2)	1063 (1)	1559 (1)	2.7
Co3	−4222 (2)	1717 (1)	571 (1)	2.7
P	−7409 (3)	2803 (2)	300 (2)	2.7
O1	−2766 (14)	2351 (10)	4046 (8)	7.2
O2	−1466 (15)	3475 (9)	2273 (9)	7.6
O3	−799 (12)	855 (8)	2865 (10)	6.2
O4	−4594 (13)	3948 (7)	2213 (9)	6.1
O5	−3464 (13)	322 (8)	3243 (8)	6.4
O6	−1622 (10)	1837 (9)	862 (8)	5.7
O7	−7064 (13)	−55 (8)	957 (10)	7.3
O8	−5351 (14)	1472 (8)	−1303 (8)	6.3
O9	−5924 (13)	1922 (7)	2595 (8)	5.5
O10	−3576 (12)	36 (7)	910 (9)	5.2
O11	−4343 (12)	3412 (7)	228 (8)	5.0
C1	−2851 (16)	2252 (10)	3384 (10)	4.1
C2	−2009 (15)	2927 (11)	2292 (10)	4.5
C3	−1569 (14)	1306 (10)	2648 (10)	4.0
C4	−4824 (14)	3374 (9)	1842 (9)	3.2
C5	−3982 (14)	641 (9)	2595 (10)	3.8
C6	−2612 (14)	1827 (10)	816 (10)	3.8
C7	−6283 (14)	400 (9)	1168 (10)	3.8
C8	−4956 (15)	1563 (8)	−575 (9)	3.5
C9	−5625 (13)	1887 (8)	2050 (10)	3.2
C10	−4040 (12)	612 (8)	984 (9)	2.6
C11	−4563 (14)	2858 (9)	511 (10)	3.7
C110	−8444 (12)	1959 (7)	−161 (8)	2.6
C111	−8205 (13)	1409 (9)	−643 (10)	3.5
C112	−8979 (15)	764 (9)	−1000 (9)	3.6
C113	−9949 (15)	625 (9)	−853 (11)	4.0
C114	−10210 (16)	1151 (10)	−370 (11)	4.4
C115	−9492 (17)	1803 (9)	−18 (11)	4.3
C120	−7584 (14)	3412 (9)	−616 (10)	3.3
C121	−8122 (16)	3170 (10)	−1471 (11)	4.1
C122	−8140 (20)	3668 (13)	−2102 (12)	5.7
C123	−7672 (25)	4384 (15)	−1908 (15)	7.6
C124	−7112 (21)	4640 (12)	−1061 (15)	6.5
C125	−7089 (20)	4165 (11)	−425 (13)	5.7
C130	−8277 (13)	3387 (8)	729 (9)	2.9
C131	−9425 (15)	3755 (12)	151 (11)	4.8
C132	−10156 (18)	4102 (10)	469 (14)	5.5
C133	−9800 (19)	4119 (11)	1338 (14)	5.3
C134	−8656 (20)	3771 (14)	1912 (13)	6.2
C135	−7902 (15)	3402 (11)	1602 (10)	4.2

^{a} $B_{eq} = {}^4/_3(\beta_{11}a^2 + \beta_{22}b^2 + \beta_{33}c^2)$.

Crystallographic Data. A violet cubic-shaped crystal of 8 with dimensions 0.17 × 0.11 × 0.22 mm was selected and sealed in a Pyrex glass capillary. Intensity data were measured on an automatic Rigaku four-circle diffractometer using LiF-monochromated Mo Kα radiation (λ = 0.71069 Å). A summary of crystal and intensity data is presented in Table V. The intensity data were measured by the $2\theta-\omega$ scan mode with a scan range of 1.0 + 0.45 tan θ. Background counts were measured for 10 s at the both end of the scan range. Four standard reflections were monitored every 50 reflections to check any unfavorable effects, but no significant change of intensities was observed throughout the data collection. The intensities of 9418 unique reflections were measured out of $2\theta = 60.0°$. A total of 3980 reflections with $F_o > 3\sigma(F_o)$ were used for the subsequent structure determination and refinement where Lorentz–polarization and analytical absorption corrections were made.

Determination and Refinement of the Structure.[22] The crystal structure was determined by conventional Patterson synthesis to locate the ruthenium atom. Fourier synthesis were then carried to locate the remaining atoms except the hydrogen atoms. The positional parameters were refined by the block-diagonal least-squares technique. The atomic scattering factors were taken from ref 23. In the final refinements, the R_1 and R_2 values were 0.0801 and 0.101, respectively. The quantity $w(|F_o| - |F_c|)^2$ was minimized, and the weighting scheme was $w^{-1} = 6.0 + 0.1|F_o|$ for $|F_o| < 40.0$ and $w^{-1} = |F_o| + 0.1|F_o|^2$ for $|F_o| > 40.0$.

---

(22) The UNICS program for M-680H computers are employed at Tokyo University Computer Centre: Sakurai's RSLC-3 lattice constant program, Ueda's PAMI Patterson program, Iwasaki's ANSFR-2 Fourier synthesis program, Ashida's HBSL-4 block-diagonal least-squares program, modified Johnson's ORTEP thermal ellipsoid plot program, and diagonal least-squares program in the X-ray system's program made by Steward et al.

(23) (a) Cromer, D. T.; Weber, J. T. *International Tables for X-Ray Crystallography*; Kynoch: Birmingham, England, 1974; Vol. 4, Table 2.20. (b) Cromer, D. T.; Liberman, D. *Ibid.*, Table 2.3.1.

Organometallics 1988, 7, 1613-1624

The standard deviation of an observation unit weight defined as $[\sum(|F_o| - |F_c|)^2/(m - n)]^{1/2}$ was 3.70, where the number of reflections (m) was 3980 and the number of refinement parameters (n) was 467. The positional parameters obtained from the last cycle of refinement were listed in Table VI with the associated standard deviations estimated from the inverse matrix. Anisotropic thermal parameters for non-hydrogen atoms and a listing of the observed and calculated structure amplitudes are available as supplementary material.[24]

---

(24) See paragraph at the end of this paper regarding supplementary material.

Acknowledgment. We thank Dr. T. Tanase for helpful discussion on X-ray crystallographic study.

Registry No. 1, 24013-40-9; 2, 105536-94-5; 3, 105560-54-1; 4, 114378-02-8; 5, 114378-03-9; 6, 114378-04-0; 7, 114394-74-0; 8, 105536-96-7; 9, 101299-76-7; 10, 105059-23-2; Ru, 7440-18-8; Co, 7440-48-4.

Supplementary Material Available: A listing of anisotropic displacement parameters for non-hydrogen atoms (1 page); a listing of observed and calculated structure factors (10 pages). Ordering information is given on any current masthead page.

Synthesis, Structures, and Solution Dynamics of Mononuclear and Dinuclear (η^5-Indenyl)rhodium Complexes of Octafluorocyclooctatetraene. Crystal and Molecular Structures of $[Rh(\eta^5\text{-}C_9H_7)(1,2,5,6\text{-}\eta\text{-}C_8F_8)]$, $\{[Rh(\eta^5\text{-}C_9H_7)]_2[\mu\text{-}(1,5,6\text{-}\eta{:}2\text{-}4\text{-}\eta\text{-}C_8F_8)](Rh\text{-}Rh)\}$, $\{[Rh(\eta^5\text{-}C_9H_7)]_2[\mu\text{-}(1,5,6\text{-}\eta{:}2\text{-}4\text{-}\eta\text{-}C_8F_7H)](Rh\text{-}Rh)\}$, and $\{[Rh(\eta^5\text{-}C_9H_7)(CO)][Rh(\eta^5\text{-}C_9H_7)][\mu\text{-}(1,2,5,6\text{-}\eta{:}7,8\text{-}\eta\text{-}C_8F_8]\}$

Richard T. Carl,[1a,2] Russell P. Hughes,*,[1a] Arnold L. Rheingold,[1b] Todd B. Marder,[1c] and Nicholas J. Taylor[1c]

Departments of Chemistry, Dartmouth College, Hanover, New Hampshire 03755, University of Delaware, Newark, Delaware 19716, and The Guelph-Waterloo Centre for Graduate Work in Chemistry, Waterloo Campus, Department of Chemistry, University of Waterloo, Waterloo, Ontario N2L 3G1, Canada

Received November 16, 1987

The molecular structure of (indenyl)(1,2,5,6-η-octafluorocyclooctatetraene)rhodium (5) has been determined. The crystal is triclinic, $P\bar{1}$, with a = 8.445 (1) Å, b = 8.850 (1) Å, c = 10.142 (1) Å, α = 85.22 (1)°, β = 81.63 (1)°, γ = 89.35 (1)°, V = 747.3 (2) Å^3, and Z = 2. Analysis of the solid-state structure in terms of the degree of slip folding of the indenyl ligand indicates that the indenyl ligand is partially slipped toward η^3-coordination and that octafluorocyclooctatetraene (OFCOT) is a slightly better acceptor ligand than ethylene. The slippage of the indenyl ligand in solution has also been analyzed from the $^{13}C\{^1H\}$NMR spectral data for 5. Line-shape analysis of the variable-temperature ^{19}F NMR spectrum of 5 allows a value of E_a for indenyl rotation of 8.6 ± 0.8 kcal/mol to be calculated. Similar variable-temperature ^1H NMR studies of the hydrocarbon analogue $Rh(C_9H_7)(1,2,5,6\text{-}C_8H_8)$ (10) produce an E_a for indenyl rotation of 9.4 ± 0.7 kcal/mol. Reaction of 5 with $Rh(C_9H_7)(C_2H_4)_2$ (9) produces the red dinuclear complex 12 whose solid-state molecular structure has also been determined by single-crystal X-ray diffraction: monoclinic, $P2_1/c$, a = 8.170 (1) Å, b = 13.770 (1) Å, c = 20.079 (3) Å, β = 96.22 (1)°, V = 2245.6 (5) Å^3, Z = 4. Solution studies of 12 using variable-temperature ^{19}F NMR indicate that the bridging OFCOT ligand is fluxional via a process (E_a = 16.3 ± 0.4 kcal/mol) which interchanges the two enantiomorphs of 12, by pairwise exchange of fluorine environments without concomitant interchange of the two rhodium environments. A mechanism consistent with these observations is proposed. The rhodium-rhodium bond in 12 is cleaved by CO to produce a mixture of 18 (major isomer) and 19 (minor isomer) and by C_2H_4 to produce the analogous complex 20. Complexes 18-20 revert to 12 thermally and are probably good models for the intermediate en route to formation of 12 from 5 and 9. The molecular structure of 18 has been confirmed by a single-crystal X-ray diffraction experiment: triclinic, $P\bar{1}$, a = 8.947 (1) Å, b = 9.840 (3) Å, c = 14.081 (3) Å, α = 96.94 (2)°, β = 102.11 (2)°, γ = 97.63 (2)°, V = 1187.2 (4) Å^3, Z = 2. Complex 12 also undergoes a kinetically selective fluorine for hydrogen exchange reaction during chromatography on various supports. The structure of the principal product 21 has also been determined crystallographically: monoclinic, $P2_1/c$, a = 11.375 (3) Å, b = 14.277 (3) Å, c = 14.211 (3) Å, β = 104.55°, V = 2233.8 (9) Å^3, Z = 4.

Introduction

The coordination chemistry of cyclooctatetraene (COT) and many of its hydrocarbon relatives has been thoroughly studied and has resulted in the synthesis of molecules that have provided an increased understanding of bonding and dynamic behavior of coordinated hydrocarbons.[3] We have been studying the transition-metal chemistry of the fluorocarbon analogue octafluorocyclooctatetraene (OFCOT)

---

(1) (a) Dartmouth College. (b) University of Delaware. (c) University of Waterloo.

(2) Present address: Nicolet Analytical Instruments, 5225 Verona Road, P.O. Box 4508, Madison, WI 53711-0508.

(3) For reviews of the organic and organometallic chemistry of cyclooctatetraene see: Fray, G. I.; Saxton, R. G. *The Chemistry of Cyclooctatetraene and Its Derivatives*; Cambridge University Press: Cambridge, 1978. Deganello, G. *Transition Metal Complexes of Cyclic Polyolefins*; Academic: New York, 1979.

0276-7333/88/2307-1613$01.50/0